Morphology and Enzymatic Degradation of Solution-Grown Single Crystals of Poly(ethylene succinate)

Tadahisa Iwata* and Yoshiharu Doi

Polymer Chemistry Laboratory, RIKEN Institute, 2-1 Hirosawa, Wako-shi, Saitama 351-0198, Japan

Keiichi Isono and Yasuhiko Yoshida

Department of Applied Chemistry, Faculty of Engineering, Toyo University, Kujirai, Kawagoe-shi, Saitama 350-8585, Japan

Received May 18, 2001; Revised Manuscript Received July 14, 2001

ABSTRACT: Solution-grown lamellar single crystals of poly(ethylene succinate) (PES) were prepared from a 0.025% solution of monochlorobenzene under an isothermal crystallization condition. Lozenge-shaped lamellar crystals with and without spiral growth were obtained at different crystallization temperature. The crystals produced well-resolved electron diffractograms. Polyethylene decoration of the crystals resulted in a "cross-sector" surface morphology and showed that the average direction of chain-folding is parallel to the crystal growth planes. In some cases, the lamellar crystals showed spiral growths originating from screw dislocations with both left-handed and right-handed forms. Two extracellular poly(hydroxybutyrate) (PHB) depolymerases purified from *Alcaligenes faecalis* T1 and *Pseudomonas stutzeri* YM1006 were used for the enzymatic degradation of the PES lamellar crystals. Adsorption of both the extracellular PHB depolymerases onto the crystal surface was observed using immuno-gold labeling technique. The enzyme molecules were homogeneously distributed on the surface of PES lamellar crystals. When the extracellular PHB depolymerase from *A. faecalis* T1 was applied to a suspension of PES crystals, the turbidity of crystal suspension did not decrease. This indicated that the *A. faecalis* T1 depolymerase could not degrade the PES crystals even though it can adsorb onto the crystal surface. On the other hand, enzymatic hydrolysis by the extracellular PHB depolymerase from *P. stutzeri* YM1006 was confirmed by the decrease in turbidity. The degradation progressed from the edges of the lamellar crystals without decreasing the molecular weights and the lamellar thicknesses. The difference in enzymatic activity seems to be due to the recognition of the distance between ester bonds in molecular chain by the active site of the enzyme molecule.

Introduction

The earliest X-ray diffraction works on the crystal structures of the type $-(-O-(CH_2)_x-O-CO-(CH_2)_y-CO-)_n-$ were done by Fuller and his collaborators.[1−4] They investigated a series of ethylene glycol polyesters with different dibasic acids. Subsequent works by many research groups included not only polyesters of ethylene glycol but also tetramethylene glycol series where both crystal structure and biodegradability were well investigated.

X-ray diffraction study of poly(ethylene succinate) (PES; $x = 2$, $y = 2$) was first studied by Fuller and Erickson, and a monoclinic unit cell with dimensions $a = 0.905$ nm, $b = 1.109$ nm, c(fiber axis) $= 0.832$ nm, and $\beta = 102.8°$ was proposed.[1] They also proposed a molecular model with a $(TG\bar{T}\bar{G})_2$ chain conformation, in which the CH_2-CH_2 bonds in the glycol and acid parts are in the form of either right-handed (G) or left-handed gauche ($\bar{G}$) while the other bonds are in the trans form (T). Bunn suggested that the chain conformation of $(TG)_2(T\bar{G})_2$ is also eligible by considering the fiber repeat distance and nonbonded atomic distances.[5] The crystal and molecular structures of PES were determined by Ueda et al.[6] which gave rise to a slight modification of the crystallographic data. PES crystallized as a *Pbnb*-D_{2h}^{10} space group with unit cell parameters $a = 0.760$ nm, $b = 1.075$ nm, and c(fiber axis) $= 0.833$ nm, and four molecular chains pass through the unit cell. On the basis of this, a new $T_3GT_3\bar{G}$ chain conformation for PES was proposed. The R factor was finally improved to 13%, and the final atomic coordinates and thermal parameters were proposed.[6] Recently, Ichikawa et al. reported the crystal modification of strained PES fiber. This modification was recognized as β-form found to be 0.95 nm fiber repeat period, which is slightly smaller than the calculated fiber repeat period for the all-trans T_8 conformation.[7,8]

Despite detailed investigations of the crystal structures and conformations of PES, morphological study on solution-grown crystals using electron microscopy has not been reported previously. Furthermore, electron diffraction of single crystals is considered as a possible approach for the understanding of modifications in crystal structures. In the chemical or enzymatic hydrolysis of biomaterials, the distribution of crystal regions and lamellar crystal size as well as the crystal morphology and structure may play a decisive role in the rate of hydrolysis. Single crystals are considered as a useful model substrate to elucidate the mechanism of enzymatic degradation of crystal region. Enzymatic degradations of single crystals of various samples have been performed. In the field of polysaccharide, single crystals of $\beta(1\rightarrow4)$xylan,[9] nigeran,[10] and $\beta(1\rightarrow4)$mannan[11] have been subjected to degradation by xylanases, mycodextranase, and mannanases, respectively. In the field of biodegradable aliphatic polyesters, various types of extracellular PHB depolymerases have been used to

* To whom all correspondence should be addressed. Tel +81-48-467-9586; Fax +81-48-462-4667; E-mail tiwata@postman.riken.go.jp.

10.1021/ma010865c CCC: $20.00
Published on Web 09/08/2001

study the degradation of single crystals of poly([*R*]-3-hydroxybutyrate) (P([*R*]-3HB))[12−18] and its copolymer[19−21] as well as poly(β-propiolactone) (PPL)[22] single crystals. The degradation of poly(L-lactic acid) (PLLA)[23] single crystals has been studied using proteinase K.

In this paper, we have attempted to obtain more insight into the structure and morphologies of PES crystals grown from dilute solution and into the enzymatic degradation mechanism of PES single crystals by two kinds of extracellular PHB depolymerases from *Alcaligenes faecalis* T1 and *Pseudomonas stutzeri* YM1006, using transmission electron microscopy, atomic force microscopy, and gel permeation chromatography. Immuno-gold labeling technique was also adopted to visualize the adsorption of enzyme molecules on single-crystal surface.

Experimental Section

Preparation of PES Single Crystals. The poly(ethylene succinate) (PES) (number-average molecular weight (M_n) = 52 800 and polydispersity (DPI) = 1.6) sample was supplied by Showa Koubunshi Co., Ltd. The PES sample was purified by reprecipitation in methanol from chloroform solution and dried in vacuo for 1 week. A 2.5 mg sample of PES was dissolved into 10 mL of monochlorobenzene at 130 °C and maintained at this temperature for 15 min. Slow cooling was then applied until the crystallization temperature, and the solution was kept there for 12 h. The slow cooling was performed by cutting off the heating element of a silicone oil bath. The crystals were collected and washed by successive centrifugations, first with monochlorobenzene and then three times with room-temperature methanol. For enzymatic degradation, the crystals were collected by centrifugation, washed with 10 or 50 mM Tris-HCl buffer, and resuspended in the same buffer.

Enzymatic Hydrolysis with PHB Depolymerases and Its Adsorption onto PES Single Crystals. The extracellular PHB depolymerases from *Pseudomonas stutzeri* YM1006 and *Alcaligenes faecalis* T1 were purified to electrophoretic homogeneity by the methods of Ohura et al.[24] and Tanio et al.,[25] respectively. Degradation of PES single crystals was monitored using a turbidimetric assay, and adsorption of extracellular PHB depolymerase on single crystals was examined using an immuno-gold labeling technique, according to the method in our previous reports.[14,15] All molecular weight data of single crystals before and after enzymatic degradation were obtained by gel permeation chromatography (GPC) using polystyrene standards of low polydispersities.[15] The water-soluble products produced during the enzymatic degradation were analyzed by using a Millennium 486 system (Waters) with a column system of Shodex OHpak SB-804 (Showadenko K. K., Tokyo, Japan) and Superdex peptide (Amersham Pharmacia Biotech), according to the method reported by Tabata et al.[26]

Transmission Electron Microscopy. Drops of PES crystal suspension, before and after enzymatic degradation, were deposited on carbon-coated grids, allowed to dry, and then shadowed with Pt−Pd alloy. For electron diffraction purposes, the dried crystals were used directly without further treatments. Small drops of PES crystal suspension, with and without gold labeling, were placed on carbon-coated grids and then allowed to dry. The decoration of single crystals with polyethylene was performed by evaporating polyethylene on the crystals under vacuum according to the method described by Wittmann and Lotz[27] and then shadowed with Pt−Pd alloy. The grids were observed with a JEM-2000FX II electron microscope operated at an acceleration voltage of 120 kV for both electron diffraction and imaging of shadowed crystals. Calibration of the patterns was done at room temperature, after depositing the crystals on gold-coated grids. Electron diffraction diagrams and images were recorded on Kodak SO-163 and 4489 films, respectively, developed for 4 min with a Kodak D19 developer (diluted in water 1/2, v/v).

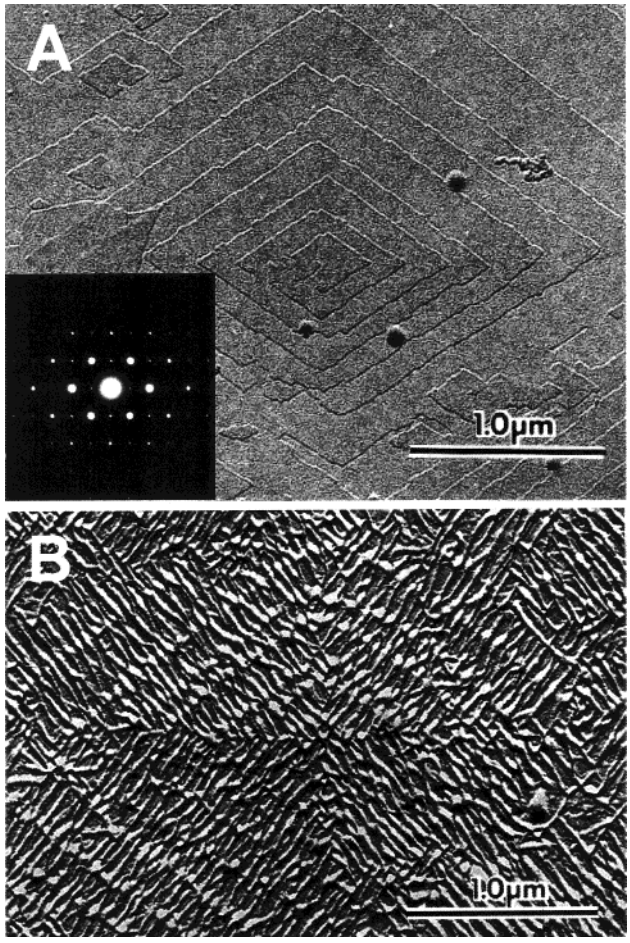

Figure 1. (A) Electron micrograph of the PES lamellar single crystals with lozenge-shaped grown from monochlorobenzene at 50 °C, after shadowing with Pt−Pd alloy. Inset: selected-area electron diffraction diagram. (B) Typical electron micrograph of lozenge-shaped PES lamellar single crystals decorated with polyethylene and shadowed with Pt−Pd alloy.

Atomic Force Microscopy. The thicknesses of PES single crystals, before and after enzymatic degradation, were investigated on the basis of atomic force microscopy (AFM). AFM measurement was performed with a SPI3700/SPA300 (Seiko Instruments Inc.). Pyramid-like Si_3N_4 tips, mounted on 100 μm long microcantilevers with spring constants of 0.09 N/m, were applied for the contact mode experiments. Simultaneous registration was performed in the contact mode for height and deflection images. Drops of crystal suspension, before and after enzymatic degradation, were deposited on mica and allowed to dry. All images were recorded at room temperature.

Results and Discussion

PES Lamellar Single Crystals. Three kinds of PES lamellar single-crystal morphologies were obtained from monochlorobenzene at different crystallization temperature. A typical electron micrograph of lozenge-shaped multilamellar crystals grown at 50 °C for 12 h is shown in Figure 1A. The ratio between the two axes of the lozenge-shaped crystal was 1:1.8, and the angles between the growth faces of a lozenge-shaped crystal are 70° and 110°. The selected-area electron diffraction diagram obtained from lozenge-shaped multilamellar crystals is an inset in Figure 1A. Each crystal yields a sharp electron diffraction diagram which contains 50 independent reflections that are mirrored in the four quadrants defined along the two orthogonal axes a^* and b^*. All the equatorial reflections of the X-ray fiber

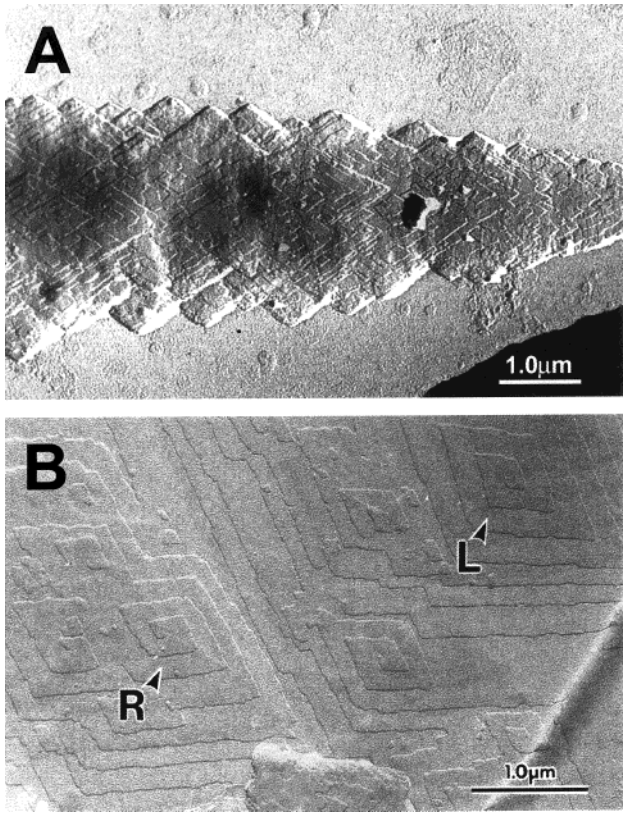

Figure 2. (A) Electron micrograph of the PES lamellar single crystals with dendritic-shaped grown from monochlorobenzene at 110 °C, after shadowing with Pt−Pd alloy. (B) Electron micrograph after shadowing with Pt−Pd alloy of lozenge-shaped PES lamellar single crystals with screw dislocations of grown from monochlorobenzene at 80 °C. Left-handed (L) and right-handed (R) screw dislocations could be observed simultaneously.

diagram reported by Ueda et al. are observed in this electron diffraction pattern, which confirms that the electron diffraction diagram is a projection along the *c*-axis; that is, the polymer chains align perpendicular to the lamellar base of the crystal. On the basis of *d*-spacing obtained from electron diffraction pattern, all reflections could be indexed by the same value of *a*-axis and the half value of *b*-axis parameters reported by Ueda et al.[6]

Figure 1B shows the PES single crystals decorated with polyethylene and shadowed with Pt−Pd alloy. Polyethylene rod crystals are oriented perpendicular to the substrate growth faces. The orientation of the decorated crystals revealed sectorization of the PES single crystal into four quadrants. This sectorized morphology was reported in polyethylene[27] and poly([*R*]-3-hydroxyvalerate) (P([*R*]-3HV))[28] single crystals that have lozenge-shaped and square-shaped morphologies. The lamellar thickness of PES lozenge-shaped crystals is about 7−8 nm as measured by AFM (image not shown). Taking the fiber repeat of 0.833 nm[1,5,6] and molecular weights into consideration, the chain-foldings occur at the lamellar surfaces of PES single crystals as is the case for biodegradable polyesters of P([*R*]-3HB),[12−18] P([*R*]-3HV),[28] PLLA,[23] etc. These results indicate that the average direction of chain-folding occurred along the lateral growth plane.

Figure 2 shows PES single crystals with various morphologies grown from monochlorobenzene at different crystallization temperature. At 110 °C, dendritic crystals as shown in Figure 2A were mainly observed. Dendritic crystals occur as multilamellar lozenge-shaped crystals with spiral growth that have a size of 0.2−0.5 μm. The thickness of the dendritic crystal is above 200 nm, indicating that it consists of many small stacked crystals. On the other hand, at a crystallization temperature of 80 °C, spiral growth crystals with right-handed or left-handed screw dislocations were observed (Figure 2B). This observation has already been reported in the cases of (*R*)- and (*S*)-poly(epichlorohydrine),[29] (*R*)- and (*S*)-poly(propylene oxide),[29] and P([*R*]-3HV)[28] single crystals. Saracovan et al.[29] and Iwata and Doi[28] have concluded that the main-chain chirality may not be involved in the determination of the handedness of screw dislocations in lamellar crystals. In the case of PES, one sees both screw dislocations on lamellar crystals as shown in Figure 2B although the molecular chain does not have any side group. This observation further supports the above conclusion. In our previous report on P([*R*]-3HV) single crystals,[28] we mentioned one possibility for the generation of both the right- and left-handed screw dislocations; that is, the helical handedness of polymer chain is the factor that contributes to the direction of screw dislocation.

Six possible PES chain conformations were reported by Fuller et al.,[1] Bunn,[5] and Ueda et al.[6] On the other hand, Yokouchi et al.[30] have proposed four energetically stable conformations for the P([*R*]-3HV) single chain. Taking into considerations the result that there was only a small difference in the potential energy among these helical handednesses, energetically, all the helical conformations could be possible. Therefore, we propose a possible explanation whereby the conformational variations of molecular chains might be involved in determining the handedness of screw dislocations in lamellar crystals grown from dilute solution at high temperature by isothermal crystallization condition.

Adsorption and Hydrolysis by Extracellular PHB Depolymerases on PES Single Crystals. Visualizations of the adsorption of extracellular PHB depolymerases purified from *Pseudomonas stutzeri* YM1006 and *Alcaligenes faecalis* T1 to solution-grown PES crystals by using anti-rabbit IgG gold conjugation are shown in parts A and B of Figure 3, respectively. Unselective distributions of extracellular PHB depolymerases on the surface of PES single crystals were observed for both *A. faecalis* T1 and *P. stutzeri* YM1006 PHB depolymerases. It was found that the concentration of adsorbed enzymes were low in both cases. In a recent study using PPL single crystals, adsorbed enzyme molecules was low compared to the concentration of enzymes that adsorbed onto P([*R*]-3HB) single crystals.[15,22] On the basis of PPL chain-folding structure calculated by the Cerius2 computer program, it was revealed that the dimethylene segment is close to the fold center and straddled by two ester units.[31] PPL and PES have no side groups in the molecular chain, and both chemical structures are very similar. Accordingly, it can be easily estimated that the ester units in the PES molecular chain do not participate in the chain-folding.

The turbidimetric degradation profile for PES single crystals by both the extracellular PHB depolymerases from *A. faecalis* T1 and *P. stutzeri* YM1006 is shown in Figure 4. In the case of *A. faecalis* T1, the turbidity of crystal suspension did not decrease despite the homogeneous adsorption of enzyme molecules onto the crystal

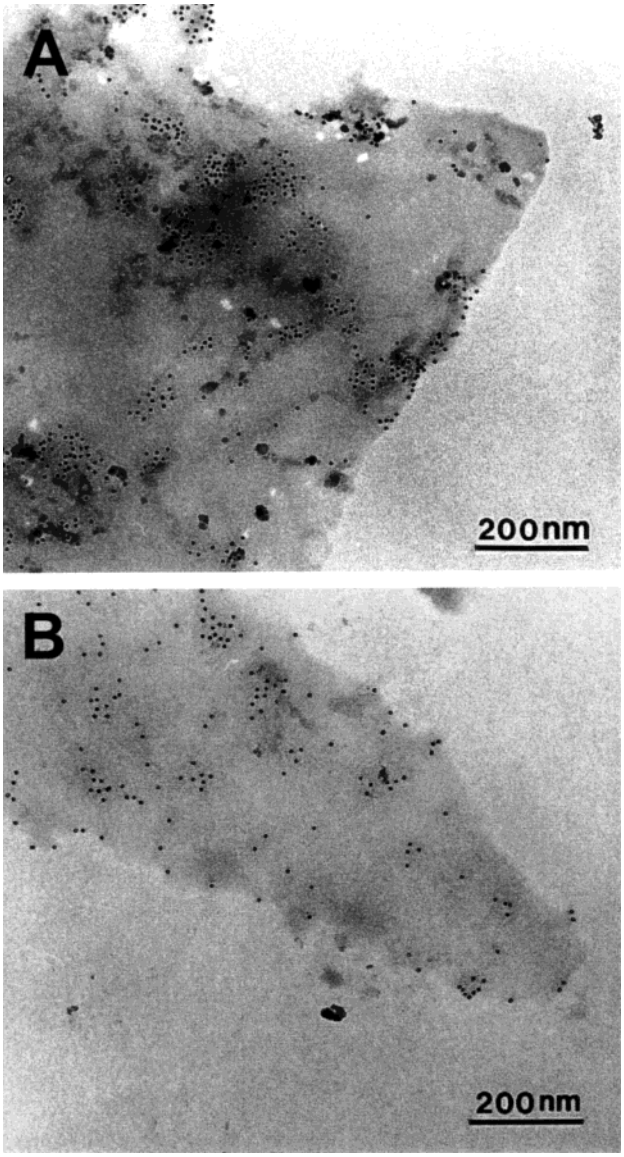

Figure 3. Visualization of the adsorption of two kinds of extracellular PHB depolymerases onto the PES lamellar single crystals (A) with *Pseudomonas stutzeri* YM1006 PHB depolymerase and (B) with *Alcaligenes faecalis* T1 PHB depolymerase, by immuno-gold labeling and transmission electron microscopy.

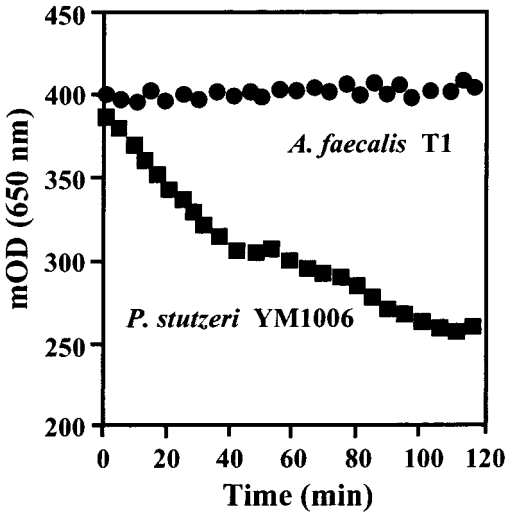

Figure 4. Turbidity of the PES crystal suspension during the enzymatic degradation, with (■) *Pseudomonas stutzeri* YM1006 and (●) *Alcaligenes faecalis* T1 PHB depolymerases.

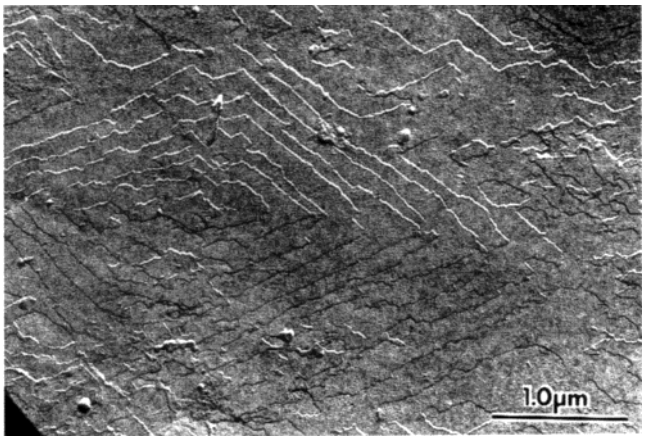

Figure 5. Electron micrograph of the PES lamellar single crystals after the partial enzymatic degradation by *Pseudomonas stutzeri* YM1006 PHB depolymerase at 37 °C.

surfaces as shown in Figure 3B. On the other hand, during the enzymatic hydrolysis using *P. stutzeri* YM1006, the turbidity decreased with time along two different lines which seem to correspond to the degradations of the loosely chain-packed regions in the crystal edges and surface and of the tightly chain-packed region.

Figure 5 shows a typical electron micrograph of PES single crystal after partial enzymatic hydrolysis by an extracellular PHB depolymerase from *P. stutzeri* YM1006. Crystals were degraded from crystal edges to form a rounded shape. When the hydrolysis proceeded further, the rounded shape became coarse and the crystal size also decreased. The remaining crystals maintained the shape of the electron diffraction patterns. On the basis of the results of both turbidity in Figure 4 and electron micrograph in Figure 5, it was found that 2 h of enzymatic attack results in a marked degradation of the PES crystals. However, the molecular weights of the crystals remained unchanged before and after enzymatic hydrolysis by the extracellular PHB depolymerase from *P. stutzeri* YM1006 (data not shown). This indicates that partial degradation at the chain-folding surfaces does not take place. In addition, AFM measurements of the PES crystals showed that the thickness of monolamellar parts also remained unchanged before and after the enzymatic degradation, providing no evidence for any enzymatic degradations from the crystal surfaces (data not shown). This phenomenon seems to be explained by three reasons: (1) the chain-folding region is not taken in the active site of the enzyme by the steric hindrance, (2) the ester units of PES molecular chain do not incorporate in chain-folding, and (3) the degradation rate of *exo*-type activity of enzyme is faster than that of *endo*-type. The same observations have been reported for the enzymatic degradation of P([*R*]-3HB] single crystals by several extracellular PHB depolymerases[12−15] and for PLLA single crystals by proteinase K.[23] The edge-attack model for enzymatic degradation of single crystals is emphasized by these results; that is, crystals are hydrolyzed mainly from the molecular chains with high mobility at the crystal periphery.

Despite the homogeneous adsorption distribution of both the enzyme molecules (*A. faecalis* T1 and *P. stutzeri* YM1006) on PES crystal surfaces, only the enzyme from

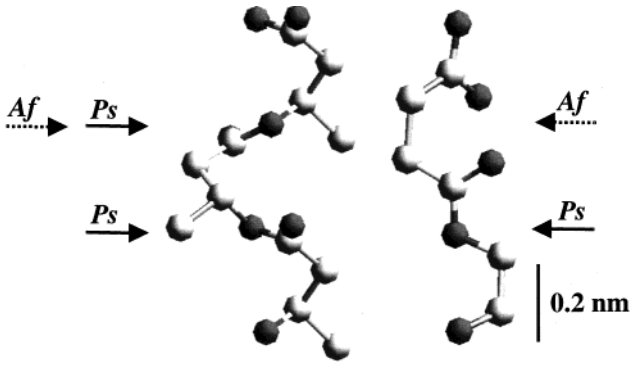

Figure 6. Molecular conformations of poly([*R*]-3-hydroxybutyrate)[35] and poly(ethylene succinate).[6] Arrows indicate the possible attack position by the active site of *Pseudomonas stutzeri* YM1006 (*Ps*, ←) and *Alcaligenes faecalis* T1 (*Af*, ← – –).

the latter can hydrolyze the PES lamellar crystals. This might be due to the recognition of the molecular residues by the active site of the enzyme molecule. Bachmann and Seebach[32] have recently reported that PHB depolymerase from *A. faecalis* T1 (PhaZafa) has four subsites in the active site, recognizing the orientation of the chain relative to its active site, and cleaves 3HB trimer and tetramer at the second ester bond from the hydroxyl terminus. A similar result was also reported by Scherer et al.[33] On the other hand, more recently, Hiraishi et al.[34] reported on the mechanism of enzymatic hydrolysis of 3HB oligomers using PHB depolymerase from *P. stutzeri* YM1006 (PhaZpst). They concluded that PhaZpst cleaves 3HB oligomer at all ester bonds and favors 3HB oligomers larger than trimer.

The enzymatic degradation of the PES single crystals by PHB depolymerase from *P. stutzeri* YM1006 produced a mixture of A-segment ($-O-CH_2-CH_2-$) and B-segment ($-O-CO-CH_2-CH_2-CO-$) of PES as water-soluble products. The GPC curves of water-soluble products after the enzymatic degradation of the PES single crystals showed three main peaks at elution times from 35 to 45 min (data not show). These peaks were identified as B-segment, A–B–A, and A–B–A–B (dimer) of PES.

Figure 6 shows the molecular conformations of P([*R*]-3HB) and PES built by using the atomic coordinates reported by Yokouchi et al.[35] and Ueda et al.,[6] respectively. The arrows indicate the possible cleavage positions of molecular chains by PhaZpst and PhaZafa. If PhaZafa attacks the second ester bond from the hydroxyl terminus as reported by Bachmann and Seebach,[32] PhaZafa cannot attack the ester bond in ethylene succinate monomer, whereas PhaZpst can hydrolyze all ester bonds. Therefore, it seems that the distance between ester bonds has to be matched with the cleavage position in the active site of the depolymerase for the cleavage of the molecular chains, in addition to the recognition of the chain orientation.

Conclusions

This paper has reported the crystal structure and morphologies of solution-grown single crystals of poly(ethylene succinate) and the visualization of enzymatic degradation of PES single crystals with the extracellular PHB depolymerases from *P. stutzeri* YM1006 and *A. faecalis* T1. Lamellar PES single crystals grown from a dilute solution of monochlorobenzene were lozenge-shaped, and at high crystallization temperature the crystals were thickened by a screw dislocation mechanism showing both left-handed and right-handed forms. The average direction of chain-folding is parallel to these growth planes as confirmed by the electron micrographs of single crystals decorated with polyethylene.

Adsorption of both the PHB depolymerases from *P. stutzeri* YM1006 and *A. faecalis* T1 on PES crystal surfaces produced a homogeneous distribution of enzyme molecules. However, in the case of *A. faecalis* T1, the turbidity of crystal suspension did not decrease. On the other hand, PHB depolymerase from *P. stutzeri* YM1006 degraded PES crystals from the edges to form a notched shape, but both the molecular weights of PES chains in crystals and the thickness of monolamellar parts remained unchanged during the enzymatic degradation. On the basis of these results, it can be emphasized that the recognition of the position of ester bonds in the molecular chain is required by the active site of the enzyme molecule for the cleavage of molecular chain.

Acknowledgment. We appreciate the assistance provided by Dr. K. Sudesh for the English correction of our manuscript. This work has been supported by a grant for Ecomolecular Science Research provided to RIKEN Institute and a Grant-in-Aid for Scientific Research on a Priority Area, Sustainable Biodegradable Plastics, No. 11217216 (2000), from the Ministry of Education, Culture, Sports, Science and Technology, Japan.

References and Notes

(1) Fuller, C. S.; Erickson, C. L. *J. Am. Chem. Soc.* **1937**, *59*, 344.
(2) Fuller, C. S.; Frosch, C. J. *J. Phys. Chem.* **1939**, *43*, 323.
(3) Fuller, C. S. *Chem. Rev.* **1940**, *26*, 143.
(4) Fuller, C. S.; Frosch, C. J.; Pape, N. R. *J. Am. Chem. Soc.* **1942**, *64*, 154.
(5) Bunn, C. W. *Proc. R. Soc. London* **1952**, *A180*, 67.
(6) Ueda, A. S.; Chatani, Y.; Tadokoro, H. *Polym. J.* **1971**, *2*, 387.
(7) Ichikawa, Y.; Washiyama, J.; Moteki, Y.; Noguchi, K.; Okuyama, K. *Polym. J.* **1995**, *27*, 1264.
(8) Ichikawa, Y.; Noguchi, K.; Okuyama, K.; Washiyama, J. *Polymer* **2001**, *42*, 3703.
(9) Chanzy, H.; Comtat, J.; Dube, M.; Marchessault, R. H. *Biopolymers* **1979**, *18*, 2459.
(10) Marchessault, R. H.; Revol, J.-F.; Bobbitt, T. F.; Hordin, J. H. *Biopolymers* **1980**, *19*, 1069.
(11) Sabini, E.; Wilson, K. S.; Siika-aho, M.; Boisset, C.; Chanzy, H. *Eur. J. Biochem.* **2000**, *267*, 2340.
(12) Hocking, P. J.; Marchessault, R. H.; Timmins, M. R.; Lenz, R. W.; Fuller, R. C. *Macromolecules* **1996**, *29*, 2472.
(13) Nobes, G. A. R.; Marchessault, R. H.; Chanzy, H.; Briese, B. H.; Jendrossek, D. *Macromolecules* **1996**, *29*, 8330.
(14) Iwata, T.; Doi, Y.; Kasuya, K.; Inoue, Y. *Macromolecules* **1997**, *30*, 833.
(15) Iwata, T.; Doi, Y.; Tanaka, T.; Akehata, T.; Shiromo, M.; Teramachi, S. *Macromolecules* **1997**, *30*, 5290.
(16) Lee, W.-K.; Iwata, T.; Abe, H.; Doi, Y. *Macromolecules* **2000**, *33*, 9535.
(17) Lee, W.-K.; Iwata, T.; Su, F.; Furuhashi, Y.; Doi, Y. *Macromol. Rapid Commun.* **2001**, *22*, 629.
(18) Murase, T.; Iwata, T.; Doi, Y. *Macromolecules* **2001**, *34*, 5848.
(19) Nobes, G. A. R.; Marchessault, R. H.; Briese, B. H.; Jendrossek, D. *J. Environ. Polym. Degrad.* **1998**, *6*, 99.
(20) Iwata, T.; Doi, Y.; Nakayama, S.; Sasatsuki, H.; Teramachi, S. *Int. J. Biol. Macromol.* **1999**, *25*, 169.
(21) Iwata, T.; Doi, Y. *Macromol. Chem. Phys.* **1999**, *200*, 2429.
(22) Furuhashi, Y.; Iwata, T.; Doi, Y. *Sen'i Gakkaishi* **2001**, *57*, 184.
(23) Iwata, T.; Doi, Y. *Macromolecules* **1998**, *31*, 2461.
(24) Ohura, T.; Kasuya, K.; Doi, Y. *Appl. Environ. Maicrobiol.* **1999**, *65*, 189.

(25) Tanio, T.; Fukui, T.; Shirakura, Y.; Saito, T.; Tomita, K.; Kaiho, T.; Masamune, S. *Eur. J. Biochem.* **1982**, *124*, 71.
(26) Tabata, K.; Abe, H.; Doi, Y. *Biomacromolecules* **2000**, *1*, 157.
(27) Wittmann, J. C.; Lotz, B. *J. Polym. Sci., Polym. Phys.* **1985**, *23*, 205.
(28) Iwata, T.; Doi, Y. *Macromolecules* **2000**, *33*, 9535.
(29) Saracovan, I.; Cox, J. K.; Revol, J.-F.; Manley, R. St. J.; Brown, G. R. *Macromolecules* **1999**, *32*, 717.
(30) Yokouchi, M.; Chatani, Y.; Tadokoro, H.; Tani, H. *Polym. J.* **1974**, *6*, 248.
(31) Furuhashi, Y.; Iwata, T.; Sikorski, P.; Atkins, E.; Doi, Y. *Macromolecules* **2000**, *33*, 9423.
(32) Bachmann, B. M.; Seebach, D. *Macromolecules* **1999**, *32*, 1777.
(33) Scherer, T. M.; Fuller, R. C.; Goodwin, S.; Lenz, R. W. *Biomacromolecules* **2000**, *1*, 577.
(34) Hiraishi, T.; Ohura, T.; Ito, S.; Kasuya, K.; Doi, Y. *Biomacromolecules* **2000**, *1*, 320.
(35) Yokouchi, M.; Chatani, Y.; Tadokoro, H.; Teranishi, K.; Tani, H. *Polymer* **1973**, *14*, 267.

MA010865C